Alkylation of Benzene with Short-Chain Olefins over MCM-22 Zeolite: Catalytic Behaviour and Kinetic Mechanism

A. Corma,*,[1] V. Martínez-Soria,† and E. Schnoeveld*

Instituto de Tecnología Química, CSIC-UPV, 46022 Valencia, Spain; and †Departament d'Engenyeria Quimica, Universitat de Valencia, 46100, Burjassot, Spain

Benzene alkylation with ethene and propene has been carried out under liquid-phase reaction conditions over zeolites MCM-22, Beta, and ZSM-5. MCM-22 seems to be a good catalyst for benzene alkylation especially with propene, showing high activity and stability and good selectivity. Kinetic experiments show that alkylation with propene follows an Eley–Rideal type mechanism. © 2000 Academic Press

Key Words: benzene alkylation with MCM-22 zeolite; benzene alkylation on Beta zeolite; cumene and ethylbenzene production on zeolites.

INTRODUCTION

Cumene and ethylbenzene are important compounds in the petrochemical industry for the production of phenol and styrene, respectively (1). Cumene and ethylbenzene are primarily produced by benzene alkylation with propene and ethene, and in the commercial processes the reactions have conventionally been catalysed by mineral acids (e.g., solid phosphoric acid) and Friedel–Crafts systems (2) (e.g., AlCl$_3$). However, economic, engineering, and environmental factors have prompted the development of new technologies in which solid acids, such as zeolite-based catalysts, are used to catalyse the direct alkylation of benzene with propene or ethene (3). In this way, several commercial processes have been developed in the past few years for the production of cumene and ethylbenzene based on zeolite catalysts (4–7). The most recent one claims the use of MCM-22 or SSZ-25 as alkylating catalysts (8–10).

MCM-22 and SSZ-25 are isostructural zeolites with the IZA code MWW. The structure is formed by two independent system of pores (11). One of the pore systems is sinusoidal with 10 MR opening and the second is defined by large 12 MR cavities (7.1 Å diameter, 18.2 Å height) connected by a single 10 MR window. These cavities are opened to the exterior at the termination of crystallites forming

chalice or cup type structures, with 12-ring openings and an approximated depth of 7 Å (12) (see Fig. 1).

In this paper we discuss the catalytic behaviour of MCM-22 for the benzene alkylation with short-chain olefins (ethene and propene) and compare it with those of Beta and ZSM-5. A mechanistic kinetic model has been developed for the alkylation of benzene with propene in order to achieve not only a kinetic expression useful for reactor design, but also a better understanding of the molecular events occurring during alkylation on zeolite MCM-22.

EXPERIMENTAL

Materials

MCM-22 samples with Si/Al = 15 and 50 were synthesised using hexamethylenimine (HM) as template following the procedure reported in Ref. (13), and starting from gels having the following compositions:

Si/Al = 15 : 0.5 HM : 44.9 H$_2$O : 0.18 Na : 0.11 OH : 0.033 Al$_2$O$_3$: SiO$_2$
Si/Al = 50 : 0.5 HM : 44.9 H$_2$O : 0.18 Na : 0.16 OH : 0.010 Al$_2$O$_3$: SiO$_2$

Commercial samples of zeolite Beta (CP811, Si/Al = 13) and zeolite ZSM-5 (CBV3020, Si/Al = 18) were used as supplied by P.Q. Corp. The nature and purity of the as-synthesized MCM-22 sample were checked by X-ray powder diffraction (Philips 1060 diffractometer). The acidity was determined by infrared spectroscopy with adsorption of pyridine and desorption at different temperatures in a Nicolet 710 FTIR apparatus following the experimental procedure described in Ref. (14). Quantitative determination of the amount of Brønsted and Lewis acid sites was derived from the intensities of the IR bands at ca. 1450 and 1545 cm^{-1}, respectively, and using the extinction molar coefficients given by Emeis (15). Textural properties of zeolites were determined from the N$_2$ adsorption–desorption experiments at 77 K on a Micromeritics ASAP-200 apparatus. The main characteristics of the zeolites are given in Table 1.

In order to determine the influence of the external surface acidity on catalytic isopropylation of benzene over

---

[1] To whom correspondence should be addressed. E-mail: acorma@itq.upv.es. Fax: 346-3877809.
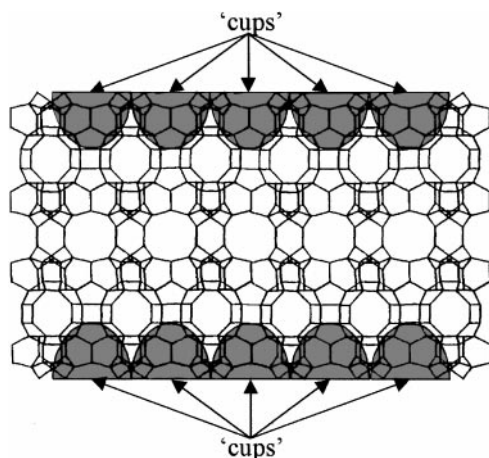
FIG. 1. MCM-22 structure, large cavities opened to the exterior at the termination of crystal (chalices).

MCM-22, a sample of MCM-22 (Si/Al = 15) was treated with 2,6-di-*tert*-butylpyridine (DTBPy) following the adsorption procedure described in Ref. 16. The presence of adsorbed DTBPy on the treated zeolite sample was checked by means of IR analysis. Previous results show that DTBPy cannot enter in the channels of MCM-22 (16), since the molecular size of DTBPy (6.3 × 8.0 Å) is too large for the molecule diffuse through 10 MR windows and channels. On this basis DTBPy was selected to passivate the external surface of MCM-22 without poisoning the internal acid site of this zeolite.

Catalytic Experiments

Alkylation of benzene with propene or ethene was performed in a computer-controlled down-flow fixed-bed stainless steel tubular microreactor, 4.1 mm i.d, 172 mm long, equipped with a 1.6 mm o.d. axial thermowell and heated by a two-zone electrical furnace. The reactor was charged with the chosen amount of catalyst always within a particle size of 0.25–0.42 mm diameter, diluted with carborundum (SiC/zeolite weight ratio = 4). The reaction conditions for catalytic test were the following: pressure, 3.5 MPa; temperature, 160–240°C; WHSV, 1.5–640 h^{-1} (referred to olefin); benzene/olefin mole ratio, 3.0–37. Under these conditions the reaction takes place in the liquid phase.

Benzene was supplied by Prolabo (A.R.). Ethene (purity >99.8%) and propene (purity >99.8%) were supplied by Abello Linde S.A. All these reagents were used without further manipulations. Preliminary alkylation experiments were carried out to ascertain that under these conditions the process was not controlled by mass transfer limitations (external and intraparticle diffusion). A small flow of nitrogen (usually <10 ml/min STP) was fed in order to improve the pressure control.

Before the alkylation reaction was started, the previously calcined (500°C) catalyst was treated at 160°C and atmospheric pressure in 100 ml/min flow of N_2 for 150 min. Then, the catalytic bed was cooled below 60°C, and benzene was fed at 2000 μl/min, increasing the pressure and temperature to the desired reaction conditions. When the desired pressure (3.5 MPa) and temperature were reached, benzene flow was adjusted to that desired for each particular experiment, and then the olefin was fed. Propene was pumped as a liquefied gas (1.5 MPa), while ethene was fed as a gas. The liquid effluent samples were collected periodically in a cold trap and analysed offline in a Varian 3350 GC equipped with an FID detector and a Supelcowax capillary column. (60 m long and 0.20 mm o.d. with a 0.20 μm thick film of stationary phase).

The MCM-22 (Si/Al = 15) sample with adsorbed DTBPy was also tested in the alkylation of benzene with propene, in order to compare the results obtained with the same sample without surface deactivation. Moreover, MCM-22 (Si/Al = 15) samples with and without DTBPy were tested for the catalytic isomerization of 1-hexene, in order to make

TABLE 1

Acidic and Textural Properties of the Catalysts

| | Si/Al ratio | Acidity,[a] μmol of pyridine/g | | | | Textural properties[c] | | | | Crystal size,[d] μm |
| | | Brønsted | | Lewis | | BET area, m^2/g | Micropore area, m^2/g | Pore volume, cm^3/g | Micropore volume, cm^3/g | |
		250°C[b]	350°C[b]	250°C[b]	350°C[b]					
MCM-22	50	25	15	13	11	461	355	0.52	0.17	0.3–0.5[e]
MCM-22	15	45	24	19	16	453	325	0.61	0.15	0.3–0.5[e]
Beta	13	36	17	47	40	509	295	0.67	0.13	0.1–0.2
ZSM-5	15	47	28	12	7	380	228	0.29	0.12	1.5–2.5

[a] Calculated using the extinction molar coefficients given by Emeis (1995).

[b] Desorption temperature.

[c] Textural properties determined using N_2 adsorption–desorption isotherms.

[d] Crystal size estimated from the SEM pictures.

[e] Hexagonal plates morphology. Average diameter.

sure that the acid sites within the micropores were not deactivated by the DTBPy adsorbed. The catalytic isomerization of 1-hexene was carried out in the gas phase under atmospheric pressure at $180°C$ using the reactor system described above. 1-Hexene, supplied by Fluka (purity $> 98\%$), was fed (2.5 ml h^{-1}) together with N$_2$ (N$_2$/hexene mole ratio = 30). The catalyst particle size was 0.25–0.42 mm mesh and the products were analysed by online GC.

RESULTS AND DISCUSSION

Alkylation of Benzene with Propene

Electrophilic alkylation of aromatics by olefins is commonly considered as proceeding via a carbenium ion type mechanism. In this way, propene is protonated by a Brønsted acid site and a carbenium ion is formed. Finally this ion is attacked by a free or weakly adsorbed benzene or isopropylbenzene (17, 18) molecule, producing cumene or diisopropylbenzene (DIPB), respectively. However, the carbenium ion formed can also react with another propene molecule, producing oligomers, which are responsible for the deactivation of the catalyst. *n*-Propylbenzene is produced in a minor amount in the reaction by secondary isomerization of cumene, which would occur via bimolecular transalkylation between cumene and benzene (19), and/or a primary product by direct alkylation of benzene with propene (20). The formation of *n*-propylbenzene is undesired since the isomer is difficult and costly to separate from the cumene stream. Cumene can also suffer a consecutive alkylation reaction, yielding diisopropylbenzenes (DIPBs). However, the DIPBs are not considered as waste products since they can be recovered by transalkylation with benzene (21).

It has been shown that Beta zeolite performs well in liquid-phase alkylation with both ethene and propene (22) and excellent efficiencies in benzene alkylation have been reported (23). Similar results have been claimed for MCM-22 zeolite in patent literature (8, 9) but there is little information available in the open literature. A recent paper (24) compares catalytic activity of MWW with Beta and other zeolites. Beta zeolite appears to be one of the most efficient catalysts and MCM-22 also shows a surprisingly good behaviour on the basis of a single experiment.

In our case, when we compare the textural and acidic properties of Beta and MCM-22 (Si/Al = 15) zeolites, it is possible to see (Table 1) that the Beta zeolite used here has a much lower Brønsted acidity, in terms of both number and strength, than the MCM-22 sample, although their nominal Si/Al ratio is very similar. The differences cannot be explained by considering only the crystallinity and structure of the samples, but it has to be assumed that a higher dealumination took place with the Beta sample during calcination. The presence of a higher amount of Lewis acid sites in Beta

zeolite, which is usually related to the presence of highly dispersed extraframework aluminium (EFAL) species formed during thermal treatment (25), supports this assumption.

The differences in textural properties, i.e., lower micropore volume and larger mesopore volume in Beta, cannot be explained only by taking into account zeolite structure. The lower microporosity and higher mesoporosity of Beta zeolite can be attributed to the agglomeration of very small crystallite size as well as a partial destruction of the zeolite lattice, which may occur during dealumination.

The catalytic activity of MCM-22 and Beta zeolites (Si/Al = 15) for the alkylation of benzene with propene was measured at different WHSV, temperature, and benzene-to-propene mole ratios (Fig. 2). It can be seen that even if both zeolites show high activity, at least at relatively short time on stream (TOS), Beta zeolite appears to have a slightly higher initial activity. Since alkylation reactions are catalysed by the acid sites of zeolites (26), we could expect that the higher the concentration of Brønsted acid sites in a zeolite the higher the alkylation activity should be. However, in this case, although MCM-22 presents a higher concentration of acid sites, its activity is slightly lower (Fig. 2a). This result can be explained by taking into account that in the case of MCM-22 only the sites pointing to the external surface, i.e., at the top and bottom of the crystallites (see Fig. 1), could allow the cumene to be formed and to diffuse out without great difficulty. Indeed, it has been reported (24) that the diffusion of cumene in the pores of MCM-22 is hampered by a high energy barrier. Moreover, it has been presented (27) by means of molecular dynamic simulation that even benzene presents a low diffusivity in either of the two pore systems of the MWW structure. On the other hand, the framework of Beta zeolite, with 12-membered ring channels, presents lower steric hindrance and both benzene and cumene can diffuse without great difficulty. Nevertheless, if the crystal size is too large, cumene diffusion can control, at least partially, the rate of the global process even in zeolites with 12 MR pores like Beta (23).

Under some reaction conditions, it can be seen (Fig. 2) that Beta deactivates faster than MCM-22, and this deactivation is faster if the B/P ratio decreases from 7.2 to 3.5 (Fig. 2d). Zeolite MCM-22 does not show deactivation, at least under the reaction conditions studied here. The deactivation in Beta zeolite can be related to the formation of propene oligomers in the channels. These species can remain strongly adsorbed and can be responsible for the observed deactivation. Since it was claimed that only the "external" acid sites are active in the case of MCM-22, the formation of oligomers in the 10 MR cavities should not affect the activity. Similar results have been obtained on SSZ-25 (10), which is isostructural with MCM-22, and it was concluded that MWW zeolite appears to be clearly superior to Beta in terms of both activity, and especially stability, when alkylating benzene with propene in a light
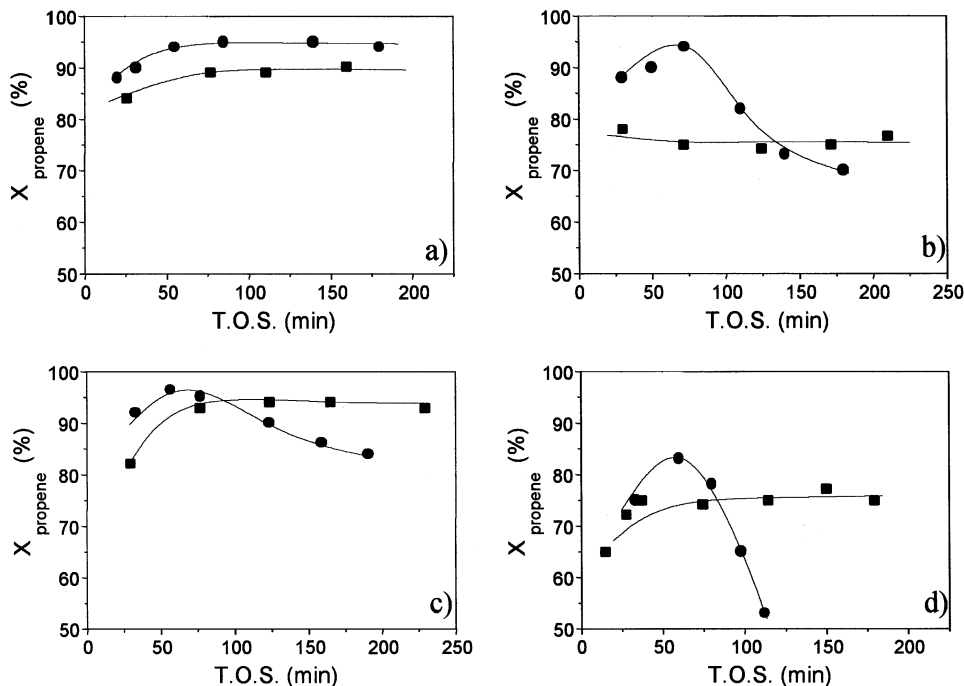
FIG. 2. Propene conversion with Beta (●) and MCM-22 (■) zeolites under the following reaction conditions: total pressure, 3.5 MPa; (a) temp, 180°C; $WHSV_{propene} = 2.6$, B/P mole ratio, 7.2; (b) temp, 180°C, $WHSV_{propene} = 5.6$, B/P mole ratio, 7.2; (c) temp, 220°C, $WHSV_{propene} = 5.6$, B/P mole ratio, 7.2; (d) temp, 200°C, $WHSV_{propene} = 11.5$, B/P mole ratio, 3.5.

reformate feedstock, but unfortunately a clear explanation for the observation was not given.

In order to explain the performance of MCM-22 we should assume that a significant number of acid sites are placed in the large "half cavities" or "chalices" opened to the exterior at the termination of the crystallites (Fig. 1). In these cavities the diffusion of the products, as well as the diffusion of the coke precursors, is easier and faster and therefore the deactivation is slower.

In order to prove the role of the external acid sites on the catalytic performance of MCM-22, the sample with Si/Al ratio of 15 was deactivated by 2,6-di-*tert*-butylpyridine (DTBPy) which has been shown to adsorb only on the ex-

ternal acid sites of this zeolite (16), while leaving untouched the acid sites within the 10 MR micropores that cannot be reached from the external surface. In agreement with previous work (16), the IR results show that DTBPy was indeed adsorbed with IR bands at 3370, 1616, and 1530 cm^{-1} which are characteristic of the DBTPyH$^+$ ion. It should be taken into account that the external acid sites that can be reached by DTBPy are only a rather small fraction of the total acid sites presented in MCM-22 (16). Then, when the sample containing adsorbed DTBPy was used to catalyse the alkylation of benzene with propene, it can be seen (Fig. 3a) that a very large decrease in activity has been produced due to the neutralisation of the most external acid
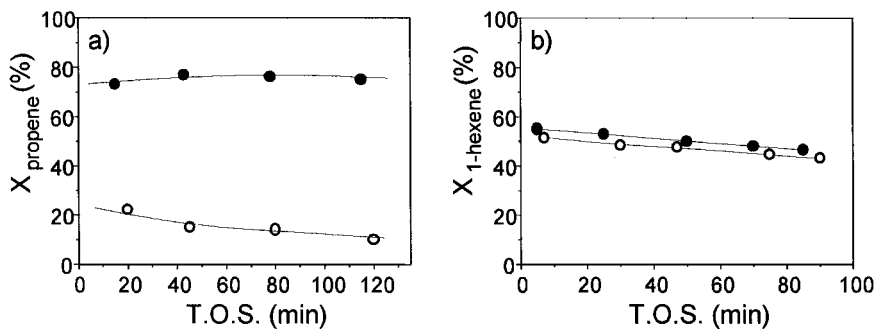

FIG. 3. Catalytic activity of MCM-22 (Si/Al = 15) without (●) and with (○) poisoning with DBTPy. (a) Alkylation of benzene with propene under the following reaction conditions: total pressure, 3.5 MPa, temp, 180°C, $WHSV_{propene} = 6.2$, B/P mole ratio, 7.0. (b) Isomerization of 1-hexene under the following reaction conditions: temp, 180°C, $WHSV_{1-hexene} = 6.6$, N$_2$/1-hexene mole ratio, 30.

sites by the bulky DTBPy. On the other hand, and in order to show that the internal acid sites were still present, the DTBPy deactivated sample was used to catalyse the isomerization of 1-hexene. This reactant was chosen because of the easy diffusion through the 10 MR windows, and also because the double bond isomerization requires low temperatures within the range of those used for the alkylation of benzene. During the isomerization of 1-hexene, the only products detected were (*cis + trans*)-2-hexene and (*cis + trans*)-3-hexene, in agreement with the reported work on the isomerization of 1-hexene on ZSM-5 (41). The results presented in Fig. 3b show that the fresh MCM-22 sample has only a slightly higher activity for 1-hexene isomerization than the sample in which the external acid sites were deactivated by DTBPy. These results are in agreement with the previous work (16) that shows that less than 10% of the total acid sites present in an MCM-22 sample can be reached from the external surface by using DTBPy. If this is the case, it has to be concluded that the alkylation of benzene by propene with MCM-22 takes place predominantly on external acid sites and/or those closer to the external surface of the crystallites.

The selectivity to the different products, as well as the distribution of the diisopropyl isomers obtained under different reaction conditions, is given in Table 2. The selectivity to cumene is quite high for both zeolites, about 90% referred to propene (>95% referred to benzene). The main secondary products observed are diisopropyl benzene isomers, *n*-propylbenzene, and propene dimerization–polymerization products, mainly hexenes (oligomers in Table 2). Often a negligible amount of other compounds, mainly alkyl aromatics, is observed. The selectivity to cumene and to oligomers decreases with increasing conversion and temperature, while the opposite occurs with respect to the selectivity of diisopropylbenzene and *n*-propylbenzene, in good agreement with previous work (28).

Although the selectivities on Beta and MCM-22 are quite similar, and no great differences are observed, it has to be pointed out that MCM-22 zeolite appears to be slightly less selective to the most undesirable products, oligomers and *n*-propylbenzene. At the lowest temperature, 180°C, MCM-22 is more selective to the formation of diisopropylbenzenes, while at the highest temperature tested, 220°C, Beta presents a higher diisopropylbenzene selectivity. This fact could be related with differences in activation energy for the transalkylation reaction between the two zeolites. On the other hand, despite the diisopropylbenzene selectivity being similar for both zeolites, there are some differences in the distributions of the different isomers as can be seen in Table 2, where is shown that the para-to-meta DIPB ratio is higher with MCM-22.

Alkylation of Benzene with Ethene

In Fig. 4, ethene conversion versus TOS for MCM-22, Beta, and ZSM-5 catalysts has been plotted. Since ethene is less reactive than propene, it was necessary to increase severity, i.e., temperature and/or contact time, in order to obtain conversion values similar to the ones obtained during propene alkylation. For the TOS considered here, deactivation is not observed with Beta and MCM-22 (Si/Al = 15), indicating that oligomerization is much lower for ethene than for propene.

ZSM-5 zeolite appears to be a poor catalyst for the alkylation of benzene with ethene in the liquid phase, and deactivates fast owing to the formation of oligomers. However, when the reaction is carried out in the gas phase ZSM-5 is one of the best catalysts for ethylbenzene production (7, 29).

Comparing Beta and MCM-22 zeolites we can conclude in general terms that the results are quite similar to those obtained in alkylation with propene; i.e., Beta is more active than MCM-22 for ethylbenzene production.

TABLE 2

Selectivity and Diisopropylbenzene Distribution Products at Different Temperature and Propene Conversions

Catalyst	Temperature, °C	X_{propene},[a] %	Selectivity,[b] %			Iso/*n*-propyl benzene ratio	DIPBs[c] distribution (%)		
			Cumene	DIPBs[b]	Oligomers		ortho	meta	para
MCM-22	180	76.05	92.12	7.34	0.32	1650	10	30	60
		97.97	90.56	9.03	0.27	830	8	32	60
	220	91.70	90.78	8.84	0.18	790	7	33	60
		96.28	89.54	9.60	0.11	460	5	38	57
Beta	180	76.25	92.16	6.96	0.41	920	6	42	52
		97.34	90.76	8.33	0.25	900	5	44	51
	220	89.90	89.34	10.07	0.21	720	5	46	49
		98.34	88.67	10.58	0.15	460	3	51	46

Note. Benzene alkylation with propene with MCM-22 and Beta zeolites. Reaction conditions: total pressure, 3.5 MPa; B/P mole ratio, 7.2. Catalyst with Si/Al ratio about 15.

[a] The different propene conversions were achieved by changing the WHSV.

[b] Selectivity referred to propene.

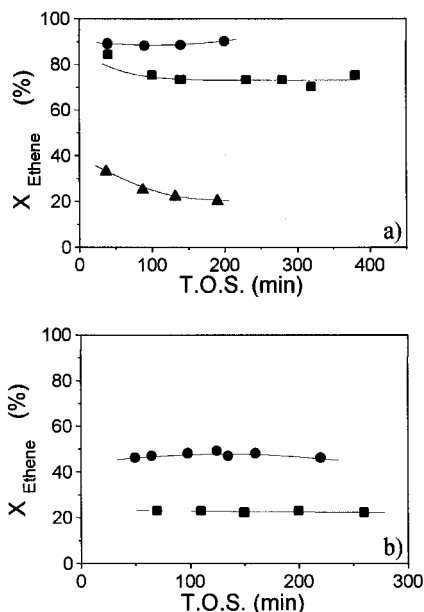[c] DIPBs: diisopropylbenzene isomers (ortho + meta + para).

FIG. 4. Ethene conversion of the different zeolites. Reaction conditions: total pressure, 3.5 MPa; (a) temp, 240°C, WHSV$_{ethene}$ = 1.2, B/E mole ratio, 8; (b) temp, 200°C, WHSV$_{ethene}$ = 6.5, B/E mole ratio, 3.0. Beta (●), MCM-22 (■), and ZSM-5 (▲).

The selectivity to the different products is shown in Table 3. MCM-22 and Beta zeolites present high ethylbenzene selectivity (~90% referred to ethene and >95% referred to benzene), while ZSM-5 presents a high proportion of butylbenzene arising from the alkylation of benzene with butene, formed by ethene dimerization. The high amount of butylbenzene formed indicates that oligomerization has proceeded quite extensively and this is responsible for the fast deactivation observed with ZSM-5.

Influence of MCM-22 Si/Al Ratio on Alkylation of Benzene with Propene and Ethene

Figure 5 shows the catalytic activity of MCM-22 samples with Si/Al ratios of 15 and 50 for the alkylation of benzene

TABLE 3

Product Selectivity in Benzene Alkylation with Ethene

Catalyst, Si/Al ≈ 15	X_{ethene}, %	Selectivity,[a] %			
		EB[a]	DEBs[b]	ButylB[c]	TEBs[d]
MCM-22	85.70	88.30	11.05	0.40	0.005
Beta	87.15	88.9	9.95	0.57	0.08
ZSM-5	31.30	42.8	3.48	51.31	0.00

Note. Reaction conditions: 240°C, total pressure, 3.5 MPa, benzene/ethene mole ratio, 9.
[a] Selectivity referred to propene.
[b] DEBs: diethylbenzene isomers (ortho + meta + para).
[c] ButylB: butylbenzene.
[d] TEBs: triethylbenzene isomers.

with propene (Fig. 5a) and ethene (Fig. 5b). As we expected, according to the concentration of acid sites (Table 1), a decrease in catalytic activity is observed when the amount of framework aluminum is decreased.

Tables 4 and 5 report the selectivities obtained in the experiments of alkylation of benzene with propene and ethene, respectively. Selectivity is expressed as mole ratio of monoalkylated cumene or ethylbenzene versus the different products. As can be seen the ratio of monoalkylated to dialkylated products is very similar for the two MCM-22 samples, indicating that at the levels of Si/Al ratio studied here the zeolite framework composition does not affect much the selectivity between mono- and dialkylated products. Nevertheless, the highest Si/Al ratio produces more oligomers (C$_6$ olefin mainly) in the alkylation with propene (Table 4) and more butylbenzene in the alkylation with ethene (Table 5). These trends suggest that the low aluminum content favours the oligomerization versus the alkylation reaction and this together with the lower concentration of acid sites on the sample with lower Al content causes this sample to deactivate faster, as can be seen in Fig. 6. Similar results were observed for Beta zeolite (23).

Finally, it is worth noting that the MCM-22 sample with the highest Si/Al mole ratio gives the highest amount of
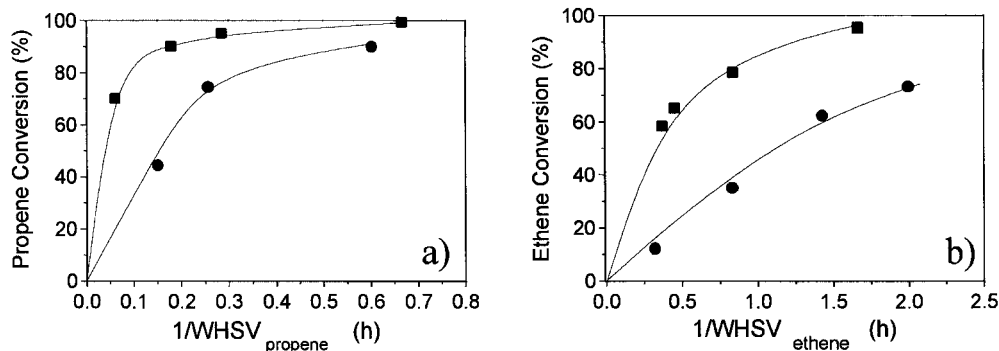

FIG. 5. Olefin conversion of the MCM-22 samples, Si/Al = 50 (●) and Si/Al = 15 (■), as a function of contact time. (a) Propene conversion at 3.5 MPa, 220°C, and B/P mole ratio 9. (b) Ethene conversion at 3.5 MPa, 240°C, and B/E mole ratio 8.

TABLE 4

Influence of MCM-22 Si/Al Ratio on Product Selectivity in Benzene Alkylation with Propene

Temperature, °C	B/P mole ratio	Conversion, %	Si/Al ratio	iPB/DIPBs[a] mole ratio	iPB/nPB[a] mole ratio	iPB/oligomers mole ratio
200	4	∼80	15	6.0	850	370
			50	6.1	620	240
220	7	∼90	15	10.1	790	500
			50	10.3	450	340

Note. Total pressure, 3.5 MPa.

[a] iPB, isopropylbenzene; DIPBs; diisopropylbenzenes; nPB, *n*-propylbenzene.

n-propylbenzene in the alkylation of benzene with propene (Table 4). An explanation for these results can be found in the differences of acid site strength distributions in the two MCM-22 samples (Table 1). Although the sample with Si/Al = 15 has more acid sites, the proportion of acid sites with medium to high strength (350°C versus 250°C pyridine desorption temperature in Table 1) is higher for the sample with the lower amount of aluminum. The higher the strength of the acid sites, the longer the average lifetime of the adsorbed species will be and consequently secondary reactions, such as the isomerization of cumene to *n*-propylbenzene, will be favoured.

Kinetics of the Alkylation of Benzene with Propene

There has been some controversy over the kinetic mechanism which can better explain the alkylation of aromatics with light olefins over acidic zeolites. While Venuto *et al.* (26) and Weitkamp (30) suggested an Eley–Rideal (ER) type mechanism for the alkylation of benzene with ethene over faujasite and ZSM-5, other authors have concluded that alkylation of benzene with short olefins follows a Langmuir–Hinselwood (LH) model (31, 32). More recently, it has been reported that the size of the pores of the zeolite can determine the alkylation mechanism (33).

In order to determine the kinetic mechanism for the alkylation of benzene with propene on MCM-22, we have carried out a kinetic study by working with a differential reactor and calculating initial rates at different benzene/propene (B/P) ratios. For all these experiments the sample used was the one with an Si/Al ratio of 15. However, since low conversion favours high olefin concentration and consequently a faster catalyst deactivation, we have measured conversion at different TOS, and from this the conversion at TOS = 0 could be determined (Fig. 7). The experiments were performed at four different temperatures, varying WHSV and benzene/propene mole ratio. The propene conversion curves as a function of contact time (1/WHSV) with different benzene/propene ratios at 220°C reaction temperature are shown in Fig. 8. Similar curves were obtained at the other temperatures studied. As the experiments were carried out with an excess of benzene and, usually, at low conversions we can make the approximation that the benzene concentration (C_b) remains practically constant.

Then if one considers the LH model and assumes that the controlling step is the propene adsorption or the chemical reaction between the adsorbed propene and benzene the

TABLE 5

Influence of MCM-22 Si/Al Ratio in Product Selectivity on Benzene Alkylation with Ethene

Temperature, °C	Conversion, %	Si/Al ratio	EB/DEB[a] mole ratio	EB/BB[a] mole ratio
240	∼70	15	11	475
		50	13	200
	∼60	15	15	375
		50	16	110
220	∼60	15	17	330
		50	18	95
	∼40	15	19	300
		50	22	75

Note. Reaction conditions: total pressure, 3.5 MPa, benzene/ethene mole ratio, 8.

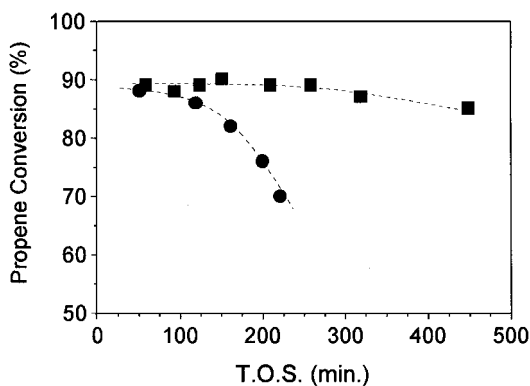[a] EB, ethylbenzene; DEB; diethylbenzene; BB, butylbenzene.

FIG. 6. Propene conversion of the MCM-22 samples as a function of time on stream, Si/Al = 50 (●) and Si/Al = 15 (■), under the following reaction conditions: 3.5 MPa, 220°C, B/P mole ratio 9, and WHSV$_{propene}$ = 1.5 and 5 for Si/Al = 50 and 15, respectively.
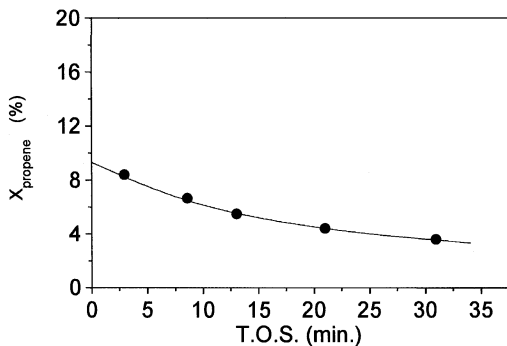
FIG. 7. Alkylation of benzene with propene over MCM-22 at low propene conversion. Reaction conditions: total pressure, 3.5 MPa, temp, 220°C, WHSV$_{propene}$ = 478, B/P mole ratio, 10.

rate of alkylation is given (34, 35) by the following equation,

$$r_a = \frac{k'_o K_a C_a}{(1 + K_a C_a + K_b C_b)^2},$$ [1]

where $k'_o = k_o$ if propene adsorption is the controlling step, or $k'_o = k_o C_b$ if the chemical reaction is the controlling step. C_a and C_b are the concentrations of propene and benzene, respectively.

If Eq. [1] is linearized it becomes

$$\frac{1}{r_a} = A_1 R + \frac{A_2}{R} + A_3,$$ [2]

where $R = C_b/C_a$ is the benzene/propene concentration ratio, and

$$A_1 = \frac{1}{k'_o K_a K_b C_b^2} + \frac{K_b}{k'_o K_a} + \frac{2}{k'_o K_a C_b}$$

$$A_2 = \frac{K_a}{k'_o K_b}$$

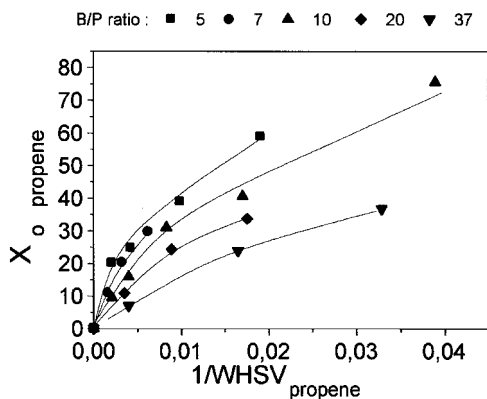$$A_3 = \frac{2}{k'_o} + \frac{2}{k'_o K_b C_b}.$$

FIG. 8. Initial propene conversion at 220°C over MCM-22 as a function of contact time for different B/P mole ratios.

On the other hand, if one considers that the reaction follows an Eley–Rideal (ER) kinetic model either with or without competitive adsorption of benzene, the following result are found:

1) Without competitive adsorption of benzene,

$$r_a = \frac{k'_o K_a C_a}{(1 + K_a C_a)}.$$ [3]

2) With competitive adsorption of benzene,

$$r_a = \frac{k'_o K_a C_a}{(1 + K_a C_a + K_b C_b)}$$ [4]

where constants have the same meaning as above.

By linearizing Eqs. [3] and [4] we arrive at the following equation,

$$\frac{1}{r_a} = A_4 R + A_5,$$ [5]

where

$$A_4 = \frac{1}{k'_o K_a C_b} + \frac{K_b}{k'_o K_a} \qquad \text{if there is benzene competitive adsorption and}$$

$$A_4 = \frac{1}{k'_o K_a C_b} \qquad \text{without benzene competitive adsorption.}$$

$$A_5 = \frac{1}{k'_o}$$

It is well known that short olefins adsorb fast and easily. Hence, what determines the kinetic behaviour is the state of benzene when it reacts with the adsorbed alkylating agent. Then if benzene reacts in an adsorbed form, the LH mechanism applies and this corresponds with Eq. [2]. On the other hand, if benzene does not react in an adsorbed form the process follows an ER kinetic expression and Eq. [5] applies.

Taking into account the continuity equation for a fixed-bed plug flow reactor (34),

$$\frac{W}{F_{a_o}} = \int_{x_a=x_a}^{x_a=0} \frac{dx_a}{r_a},$$ [6]

and that at low conversion

$$\frac{W}{F_{a_o}} \approx \frac{x_{a_i}}{r_{a_i}},$$ [7]

the following results:

$$\frac{1}{r_{a_i}} = \frac{W}{F_{a_o} x_{a_i}}.$$ [8]

By working with a differential reactor we have obtained the initial reaction rates from the tangent in the origin

TABLE 6

Initial Rate Values (r_o, mol h^{-1} g$_{cat}^{-1}$) Obtained in Alkylation of Benzene with Propene over MCM-22 (Si/Al = 15) at Different Reaction Temperatures and Benzene/Propene Mole Ratios

B/P mole ratio	Reaction Temperature			
	160°C	180°C	200°C	220°C
5	20	38	68	75
7	20	32	53	65
10	18	28	40	50
20	17	22	26	33
37	15	16	17	18

TABLE 7

Kinetic and Adsorption Constants and Standard Deviation for the Different Mechanisms

Mechanism	Constants[a]	Temperature, °C			
		160	180	200	220
RE	k_o (h^{-1})	14.4	31.3	97.9	166.7
	$\sum K_i C_b$	36.7	15.0	3.14	2.86
	σ	0.036	0.053	0.071	0.049
LH	k_o (h^{-1})	85.4	105.1	130.6	177.6
	$K_a C_b$	14.1	78.8	75.3	1084.3
	$K_b C_b$	3.9	25.5	28.2	369.2
	σ	0.050	0.067	0.086	0.062

[a] $\sigma = \sqrt{\sum (X_{\text{experimental}} - X_{\text{estimated}})^2 / (N - P)}$, where N is the number of points and p is the number of model parameters. C_b, benzene concentration.

on the curves given in Fig. 8 and the values are given in Table 6. If the benzene alkylation reaction follows an ER kinetic mechanism then the inverse of the initial reaction rate should vary linearly with the benzene/propene ratio (R parameter). On the other hand if the LH mechanism applies a convex curve should be obtained when the inverse of the initial reaction rate versus R is plotted. As can be seen in Fig. 9, the results show a good lineal correlation between $1/r_a$ and R, under the reaction conditions studied here, favouring therefore a kinetic mechanism based on an ER model. It has to be remarked that the reaction has not been studied at lower B/P ratios because (1) olefin oligomerization will dominate, (2) the reaction will not occur in the liquid phase, and (3) the assumptions made to develop the kinetic expression would not be valid anymore.

The parameter values of Eqs. [1] and [3], which are representatives of the two different mechanisms, were determined by a nonlinear optimisation method (Marquardt), integrating Eq. [6], and are given in Table 7. The quality of the fit is given by the standard deviation (σ), which is substantially lower for the ER mechanism expression for all the temperatures studied here. We can see this more clearly in Fig. 10 where it becomes apparent that ER fits better the experimental results than the LH model. Besides the fitting
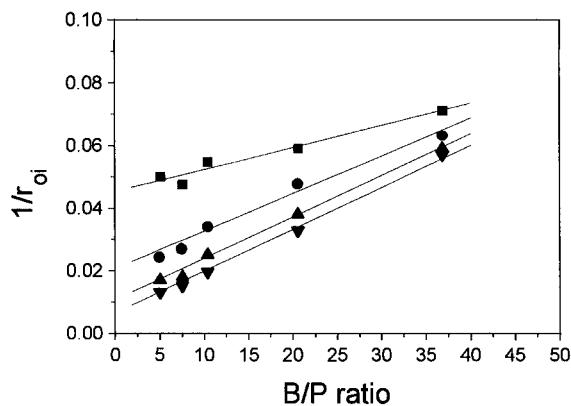
criteria, one can see that the evolution of the adsorption constants with the temperature also supports the ER model as more suitable. Indeed, the results from Table 7 clearly show that the adsorption constant values obtained from the LH and ER models increase and decrease respectively when the reaction temperature increases. Since adsorption is, generally, an exothermic process (36), taking into account the thermodynamic criteria (37), we should also favour the ER versus the LH mechanism for alkylation of benzene with propene on MCM-22 zeolite. Unfortunately, with the experimental data available we cannot determine if a competitive adsorption of benzene does or does not take place. However, taking into account the working temperatures and reported adsorption experiments (17, 38), it should be possible to say that benzene does indeed adsorb on acid sites, but the adsorption constant for benzene is much lower than the corresponding value for propene. Therefore we
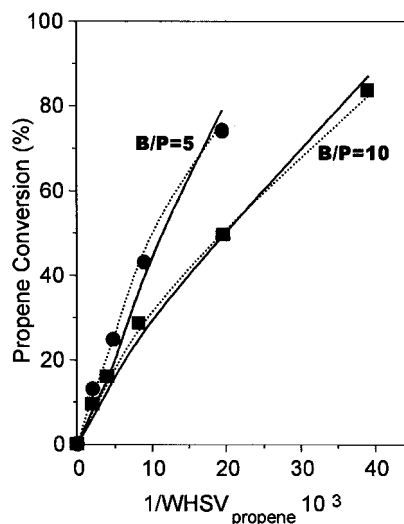
FIG. 9. Variation of initial rate with B/P ratio at different temperatures: (■) 160°C, (●) 180°C, (▲) 200°C, (▼) 220°C.

FIG. 10. Experimental (■, ●) and calculated (lines) propene conversion at 220°C over MCM-22. (···) ER model and (—) LH model.
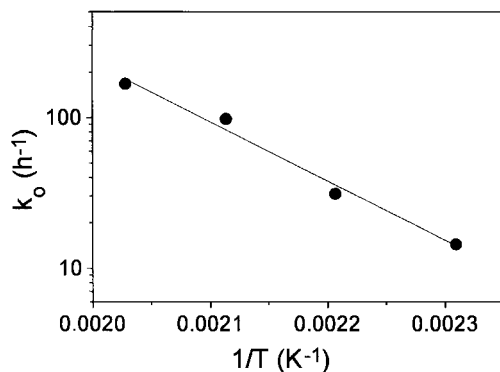
FIG. 11. Arrhenius plot for kinetic constant of the Eley–Rideal mechanism.

can conclude that while benzene is adsorbed, the product $K_b C_b$ is negligible compared to the product $K_a C_a$, and the adsorption term of the expression rate, Eq. [4], is governed mainly by the propene adsorption.

In Fig. 11 the Arrhenius plot for the kinetic rate constant is given. As we can see the fit of the experimental values to the Arrhenius equation is good, and an activation energy of 77 kJ mol^{-1} has been obtained. Values of 42 kJ mol^{-1} over an HM zeolite (32), 75 kJ mol^{-1} over an Fe-FMI zeolite (39), and 50–67 kJ mol^{-1} (40) for CaY and LaY zeolites have been reported for benzene isopropylation to cumene. The value obtained in the present work was close to the highest value of activation energy reported.

CONCLUSION

MCM-22 zeolite is a good catalyst to carry out benzene alkylation with short olefins. Comparing with a commercial Beta zeolite, MCM-22 shows similar activity and selectivity but better stability. The alkylation of benzene on MCM-22 takes place mainly on the external surface, which in this material is perfectly structured and formed by $\sim 0.7 \times 0.7$ nm cups where active sites are located. It appears then that the higher the amount of those chalices, i.e., the higher the external surface area, the better should be the catalyst for carrying out the alkylation of benzene by either propene or ethene.

From a full kinetic study it was possible to conclude that the alkylation of benzene with propene on MCM-22 follows an Eley–Rideal type mechanism in which benzene can also compete by the active sites but its coverage is much lower than that of propene.

REFERENCES

1. Pujado, P. R., Salazar, J. R., and Berger, C. V., *Hydrocarbon Process* **55**, 91 (1976).
2. Bentham, M. F., Gajda, G. J., Jensen, R. H., and Zinnen, H. A., *Erdöl Erdgas Kohle* **113**, 84 (1997).
3. Corma, A., *Chem. Rev.* **95**, 559 (1995).
4. Chen, J., Worldwide Solid Acid Process Conference, Session 3, Catalyst Consultant Inc., Houston, TX, 14–16 November 1993.
5. Meima, G. R., van der Aalst, M. J. M., Samson, M. S. V., Vossenbeerg, N. J., Adiansens, R. J. O., Garces, J. M., and Lee, J. G., Worldwide Solid Acid Process Conference, Session 3, Catalyst Consultant Inc., Houston, TX, 14–16 November 1993.
6. *Chem. Eng. News*, 18 December, 12 (1995). *Hydrocarbon Processes* October, 40 (1996).
7. Chen, N. Y., and Garwood, W. E., *Catal. Rev.-Sci. Eng.* **28**, 185 (1986).
8. Kresge, C. T., Le, Q. N., Roth, W. J., and Thompson, R. T., U.S. Patent 5,259,565, 1993.
9. Chu, P., Landis, M. E., and Le, Q. N., U.S. Patent 5,334,795, 1994.
10. Holtermann, D. L., and Innes, R., U.S. Patent 5,149,894, 1992.
11. Leonowicz, M. E., Lawton, I. A., Lawton, S. L., and Rubin, M. K., *Science* **264**, 1910 (1994). Beaumont, L. R., Vartuli, J. C., Roth, W. J., Leonowicz, M. E., Kresge, C. T., Schmitt, K. D., Chu, C. T.-W., Olson, D. H., Sheppard, E. W., McCullen, S. B., Higgins, J. B., and Schenker, J. A., *J. Am. Chem. Soc.* **114**, 10834 (1992).
12. Lawton, S. L., Leonowicz, M. E., Partridge, R. D., Chu, P., and Rubin, M. K., *Microporous Mesoporous Mater.* **23**(1–2), 109 (1998).
13. Corma, A., Corell, C., Martínez, A., and Pérez-Pariente, J., *Appl. Catal. A* **115**, 121 (1994). Corma, A., Corell, C., and Pérez-Pariente, J. *Zeolites* **15**, 2 (1995).
14. Corma, A., Fornés, V., Martínez, A., and Orchillés, A. V., *ACS Symp. Ser.* **368**, 542 (1988).
15. Emeis, C. A., *J. Catal.* **141**, 347 (1993).
16. Corma, A., Fornés, V., Forni, L., Márquez, F., Martínez-Triguero, J., and Mascotti, D., *J. Catal.* **179**, 451 (1998).
17. Venuto, P. B., and Landis, P. S., *Adv. Catal.* **18**, 259 (1968).
18. Coughlan, B., and Keane, M. A., *J. Catal.* **138**, 164 (1992).
19. Derouane, E. G., He, H., Derouane-AbdHami, S. B., and Ivanova, I. I., *Catal. Lett.* **58**, 1 (1999). Wichterlová, B., and Cejka, J., *J. Catal.* **146**, 523 (1994).
20. Bentham, M. F., Gadja, G. J., Jensen, R. H., and Zinnen, H. A., *in* "Proceeding of the DGMK Conference, Catalysis on Solid Acids and Bases, Berlin, Germany, March 14–15, 1996" (J. Weitkamp and B. Lücke, Eds.), p. 155, 1996.
21. Pradhan, A. R., and Rao, B. S., *Appl. Catal. A* **106**, 143 (1993).
22. Cavani, F., Arrigoni, V., and Bellussi, G., Eur. Pat. Appl. 432,814 A1, 1991. Innes, R. A., Zones, S. I., and Nacamuli, G. J., U.S. Patent 4,891,458, 1990. Smith, L. A., Jr., PCT Int. Appl. WO 9809929 A1, 1998. Hendriksen, D. E., Lattner, J. R., and Janssen, M. J. G., PCT Int. Appl. WO9809928 A2, 1998. Gadja, G. J., and Gajek, R. T., U.S. Patent 5,723,710, 1995.
23. Bellussi, G., Pazzuconi, G., Perego, C., Girotti, G., and Terzoni, G., *J. Catal.* **157**, 227 (1995).
24. Perego, C., Amarilli, S., Millinni, R., Bellussi, G., Girotti, G., and Terzoni, G., *Microporous Mater.* **6**, 395 (1996).
25. Corma, A., Fornés, V., Martínez, A., and Sanz, J., *ACS Symp. Ser.* **446**, 17 (1988).
26. Venuto, P. B., Hamilton, L. A., and Landis, P. S., *J. Catal.* **5**, 484 (1966).
27. Sastre, G., Catlow, C. R. A., and Corma, A., *J. Phys. Chem. B* **103**, 5187 (1999).
28. Panmig, J., Qingying, W., Chao, Z., and Yanhe, X., *Appl. Catal. A* **91**, 125 (1992).
29. Itoh, H., Miyamoto, A., and Murakami, Y., *J. Catal.* **64**, 284 (1980). Itoh, H., Hattori, T., Suzuki, K., and Murakami, Y., *J. Catal.* **79**, 21 (1983).
30. Weitkamp, J. (Int. Symp. in Zeolite Catalysis, Siofok, Hungary), *Acta Phys. Chem.* 217 (1985).
31. Morita, Y., Matsumoto, H., Kimura, T., Kato, F., and Takayasu, M., *Bull. Jpn. Pet. Inst.* **15**(1), 37 (1973).
32. Becker, K. A., Karge, H. G., and Streubel, W.-D., *J. Catal.* **28**, 403 (1973).
33. Panagiotis, G. S., and Ruckenstein, E., *Ind. Eng. Chem. Res.* **43**, 1517 (1995).

34. Froment, G. F., and Bischoff, K. B., "Reactor Analysis and Design." Wiley, New York, 1974.

35. Corrigan, T. E., Chem. Eng. January, 199 (1955).

36. Adamson, A. W., and Gast, A., "Physical Chemistry of Surfaces." Wiley, New York, 1997.

37. Rudzinski, W., and Everett, D. H., "Adsorption of Gases on Heterogeneous Surfaces." Academic Press, London, 1992.

38. Flego, C., Kiricsi, I., Perego, C., and Bellussi, G., *Stud. Surf. Sci. Catal.* **94**, 405 (1995).

39. Parikh, P. A., Subrahmanyam, N., Bath, Y. S., and Halgeri, A. B., *Can. J. Chem. Eng.* **71**, 756 (1993).

40. Allakherdieva, D. T., Romanovskii, B. V., and Topchieva, V. M., *Neftekhimiya* **9**, 373 (1968).

41. Abbot, J., Corma, A., and Wojciechowski, B. W., *J. Catal.* **92**, 398 (1985).